



# Gyre-scale deep convection in the subpolar North Atlantic Ocean during winter 2014-2015

A. Piron, V. Thierry, H. Mercier, G. Caniaux

## ► To cite this version:

A. Piron, V. Thierry, H. Mercier, G. Caniaux. Gyre-scale deep convection in the subpolar North Atlantic Ocean during winter 2014-2015. *Geophysical Research Letters*, 2017, 44, pp.1439-1447. 10.1002/2016GL071895 . insu-03682755

HAL Id: insu-03682755

<https://insu.hal.science/insu-03682755>

Submitted on 1 Jun 2022

**HAL** is a multi-disciplinary open access archive for the deposit and dissemination of scientific research documents, whether they are published or not. The documents may come from teaching and research institutions in France or abroad, or from public or private research centers.

Copyright

L'archive ouverte pluridisciplinaire **HAL**, est destinée au dépôt et à la diffusion de documents scientifiques de niveau recherche, publiés ou non, émanant des établissements d'enseignement et de recherche français ou étrangers, des laboratoires publics ou privés.

## RESEARCH LETTER

10.1002/2016GL071895

## Key Points:

- Exceptional heat loss caused exceptional convection at subpolar gyre scale during winter 2014–2015
- Exceptionally deep mixed layers directly observed south of Cape Farewell (1700 m) and in the Irminger Sea (1400 m)
- This exceptional convection was favored by and enhanced the cold anomaly that developed recently in the North Atlantic Ocean

## Supporting Information:

- Supporting Information S1

## Correspondence to:

V. Thierry,  
vthierry@ifremer.fr

## Citation:

Piron, A., V. Thierry, H. Mercier, and G. Caniaux (2017), Gyre-scale deep convection in the subpolar North Atlantic Ocean during winter 2014–2015, *Geophys. Res. Lett.*, 44, 1439–1447, doi:10.1002/2016GL071895.

Received 10 NOV 2016

Accepted 27 JAN 2017

Accepted article online 29 JAN 2017

Published online 13 FEB 2017

## Gyre-scale deep convection in the subpolar North Atlantic Ocean during winter 2014–2015

A. Piron<sup>1</sup> , V. Thierry<sup>1</sup> , H. Mercier<sup>2</sup> , and G. Caniaux<sup>3</sup> 

<sup>1</sup>Ifremer, Laboratoire d'Océanographie Physique et Spatiale, UMR 6523 CNRS-IFREMER-IRD-UBO, Plouzané, France, <sup>2</sup>CNRS, Laboratoire d'Océanographie Physique et Spatiale, UMR 6523 CNRS-IFREMER-IRD-UBO, Plouzané, France, <sup>3</sup>Centre National de Recherches Météorologiques, UMR 3589 Météo-France-CNRS, Toulouse, France

**Abstract** Using Argo floats, we show that a major deep convective activity occurred simultaneously in the Labrador Sea (LAB), south of Cape Farewell (SCF), and the Irminger Sea (IRM) during winter 2014–2015. Convection was driven by exceptional heat loss to the atmosphere (up to 50% higher than the climatological mean). This is the first observation of deep convection over such a widespread area. Mixed layer depths exceptionally reached 1700 m in SCF and 1400 m in IRM. The deep thermocline density gradient limited the mixed layer deepening in the Labrador Sea to 1800 m. Potential densities of deep waters were similar in the three basins ( $27.73\text{--}27.74 \text{ kg m}^{-3}$ ) but warmer by  $0.3^\circ\text{C}$  and saltier by 0.04 in IRM than in LAB and SCF, meaning that each basin formed locally its own deep water. The cold anomaly that developed recently in the North Atlantic Ocean favored and was enhanced by this exceptional convection.

### 1. Introduction

Deep convection is a key oceanic process that ventilates the lower limb of the Meridional Overturning Circulation (MOC), thus contributing to the storage of heat, anthropogenic carbon and oxygen in the deep ocean [Pérez *et al.*, 2013]. Monitoring and understanding variability in volumes and properties of the water masses produced by deep convection is required to better model and predict future changes in deep convection in a warming world. It would also allow a better assessment of the link between deep convection and the MOC intensity measured at mid-latitudes [Cunningham *et al.*, 2007] and subpolar latitudes [Mercier *et al.*, 2015].

The Labrador Sea Water (LSW) is formed by deep convection in the western North Atlantic Ocean subpolar gyre. In the last decades several sites of LSW production were identified, each site showing large interannual to decadal variability in convection strength. In the Labrador Sea, the deepest winter mixed layers were observed between the late 1980s and the mid-1990s [Yashayaev, 2007] due to the recurrence of severe winters during this high North Atlantic Oscillation (NAO) index period [Hurrell, 1995]. They reached 2300–2400 m in 1993–1995 [Kieke and Yashayaev, 2015]. Since the mid-1990s, the convection was shallower due to milder winters and the maximum mixed layer depths (MLDs) ranged from 500 to 1500 m, except in 2008 and 2014 when they reached 1850 and 1700 m, respectively [Våge *et al.*, 2009; Yashayaev and Loder, 2009; Kieke and Yashayaev, 2015]. Based on hydrographic data collected over the period 1900–2000, Pickart *et al.* [2003a] showed that the core of the deep convection area is localized west of  $52^\circ\text{W}$  and south of  $59^\circ\text{N}$ . The deep convection area extended to  $48^\circ\text{W}$  and  $60^\circ\text{N}$  during the deep convective years of the early 1990s [Pickart *et al.*, 2003a] and retreated westward in the early 2000s [Våge *et al.*, 2009].

In the last decade, the Irminger Sea was also recognized as a deep convection site forming LSW under favorable conditions such as positive NAO index, preconditioning of the water column, and strong heat loss to the atmosphere due to high wind speed events occurring east of Cape Farewell (the so-called Greenland Tip Jets) [Bacon *et al.*, 2003; Pickart *et al.*, 2003b; Våge *et al.*, 2009; de Jong *et al.*, 2012; Piron *et al.*, 2016]. The end of winter MLDs in the Irminger Sea reached 1000 m in 2008 and 2012 [de Jong *et al.*, 2012; Piron *et al.*, 2016] and 1400 m in 2015 [de Jong and de Steur, 2016; Fröb *et al.*, 2016], which are the deepest mixed layers observed in that region. Based on a one-dimensional (1-D) mixed layer model, Våge *et al.* [2008] and Pickart *et al.* [2003a] suggested that convection might have reached 1500–2000 m in 1994 and 1995.

South of Cape Farewell, Bacon *et al.* [2003] and Piron *et al.* [2016] observed MLDs of 900–1000 m in 1997 and 2012, respectively. While this region was considered in some studies as part of the Irminger Sea [Piron *et al.*, 2016; Bacon *et al.*, 2003], it could be a third distinct deep convection site. Indeed, using the minimum

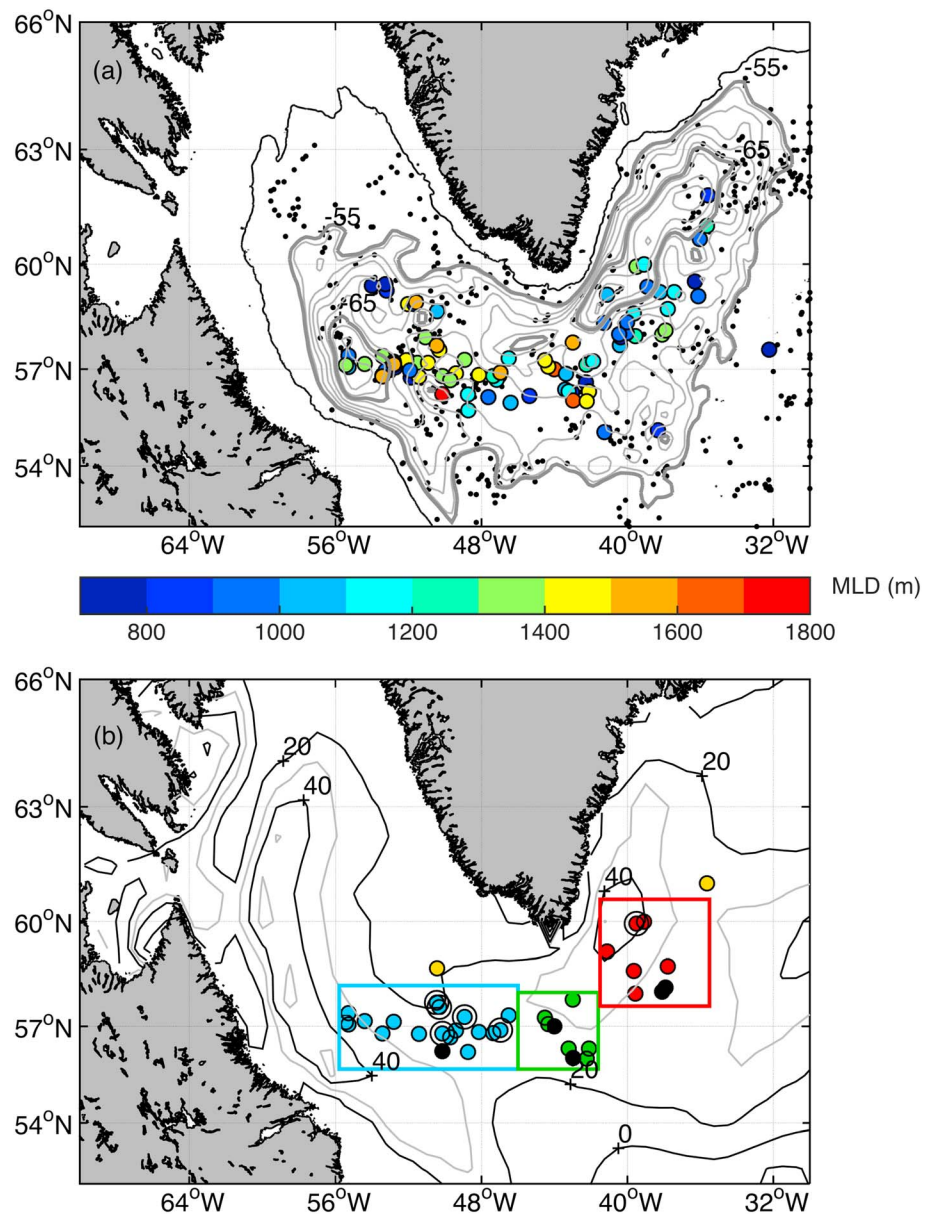


**Figure 1.** (a) Positions of Argo profiles available over January–April 2015. Black dots:  $\text{MLD} < 700 \text{ m}$ ; colored dots:  $\text{MLD} > 700 \text{ m}$ . Superimposed are the 1000 m isobath (thin black line) and the Absolute Dynamic Topography (cm) averaged over January–April 2015 (gray contours). (b) Positions of the late winter (March–April)  $\text{MLD} > 1000 \text{ m}$  in the LAB (blue dots), SCF (green dots), and IRM (red dots) boxes. Black dots: the deepest mixed layer in each box (1790, 1700, and 1400 m, respectively). Yellow dots: profiles with  $\text{MLD} > 1000 \text{ m}$  outside the boxes. Black circles: profiles with oxygen data shown in Figure 3. Black contours: winter (“DJFM) anomalies (in %) of air-sea heat fluxes relative to the 1979–2015 climatological value. Positive numbers indicate stronger than average air-sea heat loss to the atmosphere.

potential vorticity at 1000 m as a footprint of the deep convective activity, *Pickart et al.* [2003a] showed that during the 1989–1997 period there was a separate area of minimum potential vorticity south of Cape Farewell. In this latter area, a near-surface stratified layer capping a homogenous layer down to 1800 m in 1991 and 1600 m in 2008 was observed by *Pickart et al.* [2003a] and *Våge et al.* [2009], respectively. Those results suggest that MLDs could extend deeper than 1000 m south of Cape Farewell.

*Våge et al.* [2009] described the deep convection at the subpolar gyre scale for the winter 2007–2008 (winter  $(N - 1) - N$  will be referred to as Winter $N$ ) owing to Argo data. The sampling in the Irminger Sea and south of Cape Farewell was, however, insufficient to allow comparison of the deep convection properties (depth, spatial extent, and thermohaline properties) in the different convection sites and to relate them to the

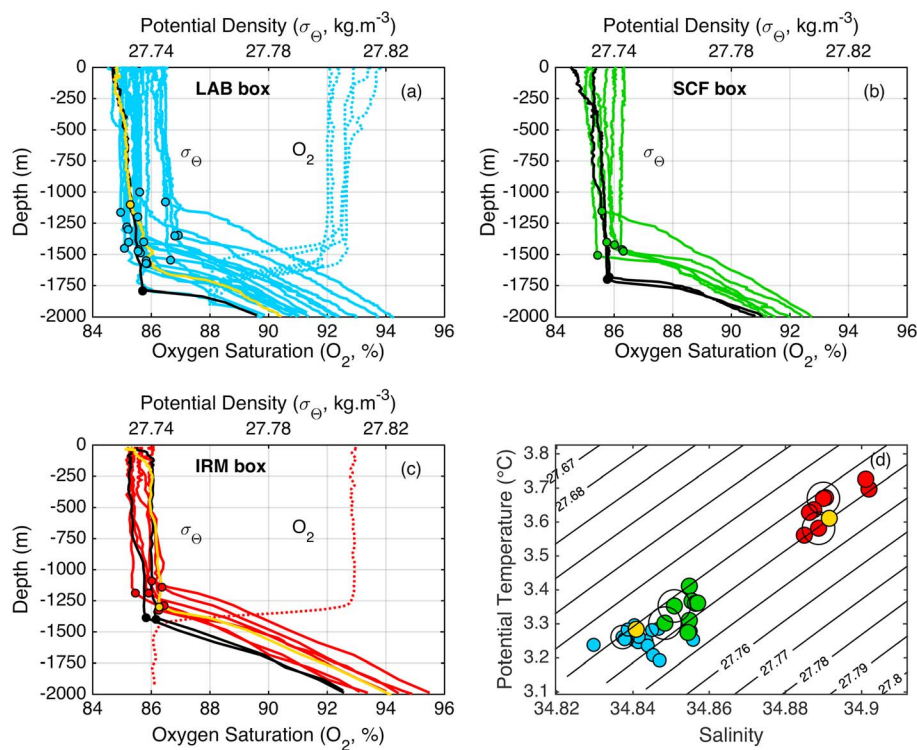


**Figure 2.** (a–c) Late winter (March–April) profiles with MLD > 1000 m in the LAB (Figure 2a), SCF (Figure 2b), and IRM (Figure 2c) boxes. Thick lines: potential density ( $\text{kg m}^{-3}$ ). Thin dashed lines: oxygen saturation (%). Black line: profiles with the deepest mixed layers. Yellow line: profile located outside the boxes. MLD is indicated with dots on the density profiles. (d) Properties of the late winter profiles with MLD > 1000 m in LAB (blue dots), SCF (green dots), and IRM (red dots). The black circles identify properties of the deepest mixed layers. The yellow dots identify profiles located outside the boxes.

atmospheric forcing and oceanic preconditioning. This is now possible for Winter15 because of an adequate Argo sampling of the subpolar gyre. The number of profiles available in the three convection sites during winter (DJFM) was 2 to 3 times larger in Winter15 than in Winter08 (183 profiles against 80). Winter15 was characterized by deep mixed layers [Fröb *et al.*, 2016] and a NAO index close to 2 corresponding to the highest value observed since the early 1990s suggesting a strong atmospheric forcing. This motivated the investigation of deep convection in the subpolar gyre for Winter15.

## 2. Data and Methods

Argo data were used to describe the mixed layers for Winter15. We selected Argo temperature, salinity, and oxygen profiles available in the subpolar gyre of the North Atlantic Ocean (52–66°N; 30°W–66°W) between 1 September 2014 and 30 April 2015 [Argo, 2015]. Oxygen data were corrected as suggested by Takeshita *et al.* [2013] by using as a reference either the oxygen profile collected at float deployment if available or the World Ocean Atlas 2009 [Garcia *et al.*, 2010]. As in Piron *et al.* [2016], MLDs were calculated for each profile by comparing the split-and-merge [Thomson and Fine, 2003] and threshold [de Boyer Montégut *et al.*, 2004] methods and a visual control. Mixed layers isolated from the surface [Pickart *et al.*, 2002] are not considered here to guarantee that the estimated MLDs correspond to mixed layers formed locally.

We used the surface wind stress, air-sea heat flux, and sea surface temperature (SST) provided by the ERA-Interim reanalysis [Dee *et al.*, 2011]. We used the Absolute Dynamic Topography (ADT) data provided by AVISO, and Sea Ice data from the National Snow and Ice Data Center (NSIDC) [Fetterer *et al.*, 2016].

## 3. The 2014–2015 Deep Convection

To characterize the deep convection of Winter15, we considered Argo profiles with MLD exceeding 700 m (MLD > 700 m) because it is the minimum depth to be reached for LSW renewal [Yashayaev, 2007;

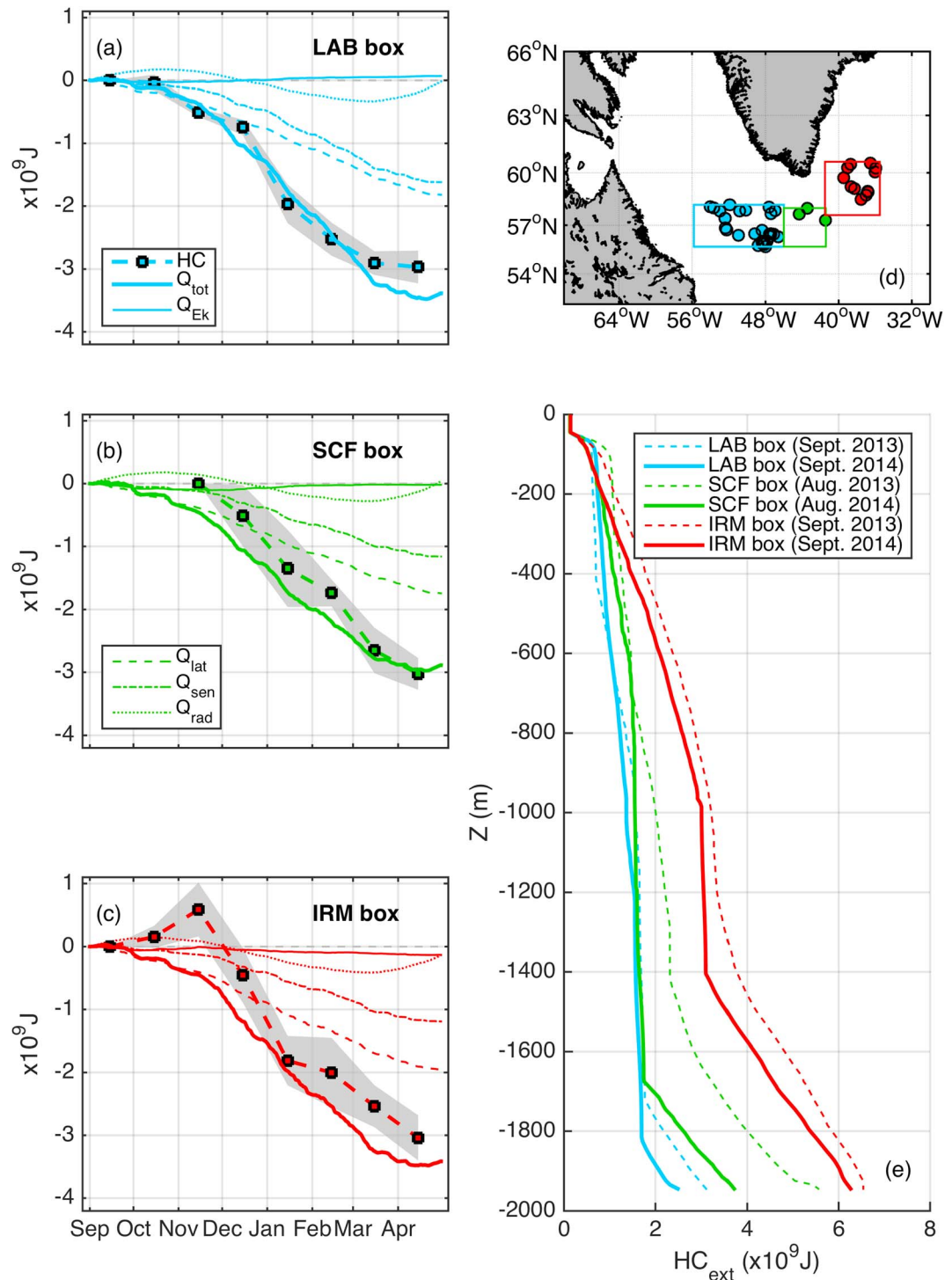


**Figure 3.** (a-c) Time series of the mixed layer heat content (HC) and associated error (gray shading) and of the cumulative sum from 1 September 2015 of the heat fluxes in LAB (Figure 3a), SCF (Figure 3b), and IRM (Figure 3c).  $Q_{tot}$  is the sum of the radiative fluxes ( $Q_{rad}$ ), latent ( $Q_{lat}$ ), sensible ( $Q_{sen}$ ), and Ekman transport heat fluxes ( $Q_{Ek}$ ). (d) Positions of the late summer profiles used to calculate a mean late summer potential temperature profile in each box. (e) Quantity of heat to extract from each box ( $HC_{ext}$ ) to homogenize this late summer profile down to depth  $Z$ .

Piron et al., 2016]. Those profiles were obtained between 24 January and 22 April 2015. They cover a continuous wide area extending from the interior of the Labrador Sea (east of  $55.4^\circ\text{W}$ ) to the Irminger Sea (west of  $32.2^\circ\text{W}$ ) (Figure 1a) and are all located within the cyclonic circulation surrounding the Labrador

and Irminger Seas as identified by the ADT contour –55 cm [Våge *et al.*, 2011; Piron *et al.*, 2016]. The spatial coverage is relatively homogeneous, and the 88 profiles with MLD > 700 m represented 23% of the profiles located within this ADT contour during January–April 2015.

In the Irminger Sea (east of 42°W), most of the MLDs varied between 1000 and 1400 m. The deepest MLDs (1400 m) were observed on 17 March and 16 April. In the Labrador Sea and south of Cape Farewell, the MLDs were deeper than in the Irminger Sea and many profiles had MLDs deeper than 1400 m. The deepest MLDs observed in the Labrador Sea and south of Cape Farewell were 1790 m (18 March) and 1700 m (15 and 29 March), respectively. To go further in the description of the convection, we considered late winter MLD > 700 m (March–April) and calculated median (Me), first (Q1), and third (Q3) quartiles for the three boxes defined in Figure 1b and referred to as LAB (Labrador Sea), SCF (south of Cape Farewell), and IRM (Irminger Sea). Fifty percent of the MLD > 700 m were deeper than 1400 m in LAB (Me = 1399 m), and 25% of them exceeded 1500 m (Q3 = 1502 m). The maximum MLD reached in LAB is similar to the deepest MLDs observed in the last decade in this area. Similar statistics were obtained for SCF (Me = 1468 m, Q3 = 1603 m) where the maximum MLD observed (1700 m) is deeper than past observations. For IRM, 75% of the MLDs > 700 m were deeper than the deepest MLD ever observed in that area (1000 m) and 25% of the profiles even exceeded 1300 m (Q1 = 995 m, Q3 = 1316 m).

Potential density and oxygen of the vertical profiles with the deepest (MLD > 1000 m) late winter MLDs were homogeneous from the surface to the base of the mixed layer (Figures 2a–2c). As argued in Piron *et al.* [2016], this testifies that the deep convection occurred locally. For those profiles, the mixed layer properties (potential temperature, salinity, and potential density) were determined at the potential vorticity minimum [Piron *et al.*, 2016]. The potential density ranged between 27.73 and 27.75 kg m<sup>-3</sup> in the three boxes (Figure 2d). The range is reduced to 27.73–27.74 kg m<sup>-3</sup> for the deepest MLDs. In IRM, the MLDs > 1000 m were warmer and saltier than in the Labrador Sea and south of Cape Farewell (3.55–3.70°C against 3.2–3.4°C; 34.88–34.90 against 34.84–34.86). The mixed layers in LAB were also slightly colder (~0.1°C) and fresher (~0.01) than those located in SCF.

To relate the formation of the deep mixed layers to the atmospheric forcing, we compared the temporal evolution of the mixed layer heat content (HC) and of the cumulative heat flux  $Q_{\text{tot}}$  split into the shortwave and longwave ( $Q_{\text{rad}}$ ), latent ( $Q_{\text{lat}}$ ), and sensible ( $Q_{\text{sens}}$ ) heat fluxes and horizontal Ekman transport heat fluxes from September 2014 to April 2015 in the three boxes (Figures 3a–3c). de Boisséson *et al.* [2010] and Piron *et al.* [2016] showed the suitability of ERA-Interim data for such comparison in the subpolar gyre of the North Atlantic Ocean. The Ekman heat flux is induced by the horizontal Ekman advection acting on horizontal temperature gradients, which are computed, following Piron *et al.* [2016], from SST data. For convenience, all terms were initialized at 0 in September. The Ekman component represented at most 10% of the total heat loss. The latent heat loss dominated in IRM and SCF and represented about 60% of the total heat loss. In LAB, the latent and sensible heat fluxes represented about half of the total heat flux each. HC was estimated from the calculation of the mixed layer heat content variation (HCV) between two consecutive months in considering a MLD equal to the maximum MLD value observed over the 2 months. The procedure is similar to that used by de Boisséson *et al.* [2010] along floats trajectories.

The temporal evolution of the mixed layer heat content is explained at first order by the sum of the air-sea and Ekman transport heat fluxes (Figures 3a–3c). The agreement between HC and  $Q_{\text{tot}}$  is striking in LAB. In IRM, the total heat loss to the atmosphere was stronger than the mixed layer heat content variations. The differences may be due to biases on the air-sea forcing and to other processes that were not taken into account like entrainment into mixed layer of water from below [Lilly *et al.*, 1999] or horizontal advection of the warm Atlantic waters from the boundary current [Lazier *et al.*, 2002]. This latter mechanism possibly explains the mixed layer warming observed in November 2014.

#### 4. Discussion

In agreement with the high NAO index characterizing Winter15, the oceanic air-sea heat loss over the subpolar gyre during Winter15 was 20% to 50% larger than the 1979–2015 climatology (Figure 1b) and 20 to 40% higher over the three convection sites. Anomalies were not due to anomalously cold (and dry) air temperature and large sea ice extent (Figure S1 in the supporting information) as in 2007–2008 [Våge *et al.*, 2009] but

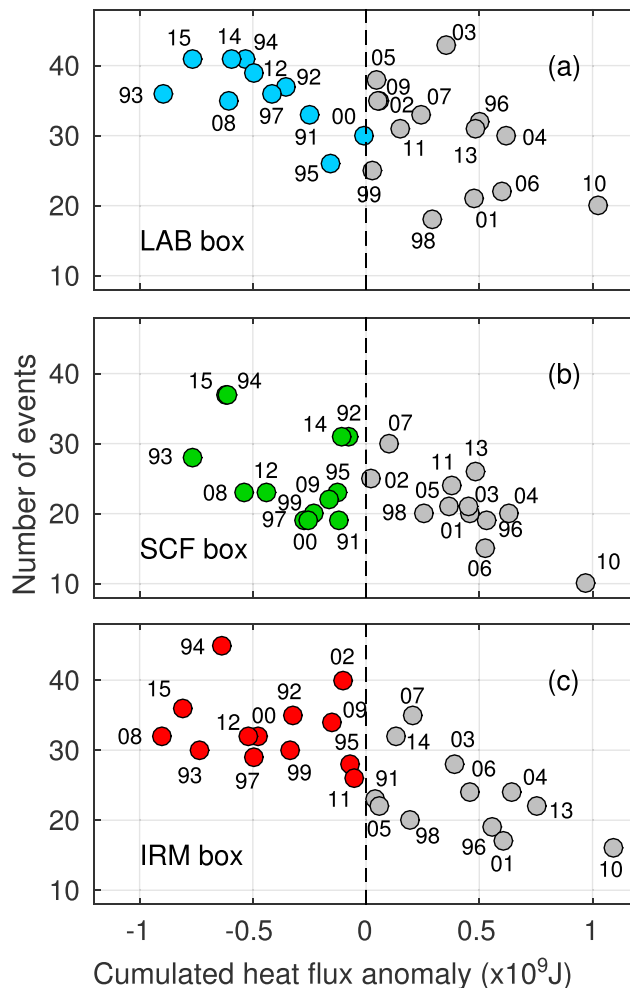


**Figure 4.** Number of strong wind events as a function of total heat flux anomalies cumulated from 1 September to the date when the net air-sea heat flux to the ocean starts to be positive. The total heat flux is the sum of air-sea and Ekman heat fluxes. Anomalies were computed relative to the climatological value estimated over 1979–2015 and equal to  $-2.6$ ,  $-2.4$ , and  $-2.7 \times 10^9 \text{ J}$  in (a) LAB, (b) SCF, and (c) IRM, respectively. Years indicated in Figures 4a–4c correspond to the year of the end of winter.

an incomparably wide region in the subpolar North Atlantic as already noted by Fröb et al. [2016].

However, the atmospheric conditions alone cannot explain why the late winter MLDs were shallower in the Irminger Sea than in the Labrador Sea and south of Cape Farewell despite similar winter heat loss amplitudes in the three boxes ( $3 \times 10^9 \text{ J}$ ; Figures 3a–3c); why the MLD deepening stopped at 800–1000 m in 2007–2008 [Våge et al., 2008; de Jong et al., 2012] while Winter08 was as exceptional as Winter15 in terms of heat loss and number of strong wind events (Figure 4); and why the exceptional air-sea forcing did not lead to exceptionally deep MLDs in the Labrador Sea. To address those questions, we assessed the role of the preconditioning of the water column for each box by computing the amount of heat that should be extracted ( $\text{HC}_{\text{ext}}$ ) from an end of summer profile to homogenize it down to a given depth (Figures 3d and 3e). The computation was carried out using mean potential temperature profiles calculated from all profiles available in September 2014 in LAB and IRM and in August 2014 in SCF because no profiles were available in this box in September (Figures 3d and 3e). This supposes that the mixed layer deepening is mainly a one-dimensional process governed by winter heat loss. This is true at first order for Winter15 (Figures 3a–3c), and this was proven to be true for other winters in the Labrador Sea [Lilly et al., 1999; Yashayaev and Loder, 2009] and in the Irminger Sea [Våge et al., 2008].

resulted from positive wind speed anomalies in the  $53$ – $63^\circ\text{N}$  latitude band associated with an intensification of the meridional surface pressure gradient [Duchez et al., 2016]. Winter15 atmospheric conditions for the three deep convection sites are further characterized by determining the number of strong wind events (Figure 4). A strong wind event was defined by a wind stress larger than 3 times the wind stress standard deviation estimated over the period 1990–2015 between 1 September and the date when the net air-sea heat flux to the ocean starts to be positive. The calculation was done in LAB, SCF, and IRM and for all winters since 1991. Note that in the Irminger Sea strong wind events correspond generally but not only to the westerly Greenland Tip Jets [Pickart et al., 2003b].

Compared to the other winters of the period 1990–2015, Winter15 was exceptional in terms of winter heat loss and strong wind event occurrences (Figure 4). For the three boxes, Winter15 is the second winter after Winter93 in terms of strong heat loss anomaly. It was also among the top three winters in terms of large number of strong wind events. Those exceptional atmospheric conditions caused the formation of exceptionally deep MLDs south of Cape Farewell and in the Irminger Sea and explain the fact that deep convection occurred over

In IRM, the  $HC_{ext}$  curve predicts a MLD of 1400 m that matches the observed maximum MLD when considering the observed Winter15 heat loss (Figure 3e). The predicted MLD corresponds also to the top of the deep thermocline that acts as a barrier for a further deepening of the MLD. A heat loss almost twice as large as the one observed during Winter15 would have been necessary to reach a MLD in the Irminger Sea as deep as those observed in the Labrador Sea (1800 m). Considering the already exceptional character of Winter15, 1400 m is obviously the deepest MLD that can be reached with the current preconditioning. By contrast, the barrier effect due to the deep thermocline was not the limiting factor for the further deepening of the mixed layers in Winter08 because, as argued by *de Jong et al.* [2012], the density gradient at the base of the end of winter mixed layers was weak. The exceptional heat loss of Winter08 in IRM (Figure 4c) removed the strong initial temperature stratification induced by the mild winters of the early 2000s. The surface cooling ceased or weakened sufficiently in March for restratification by advection of warmer waters from surrounding boundary currents to take place, and no further deepening of the mixed layers was observed [*de Jong et al.*, 2012]. In LAB and SCF, the maximum Winter15 MLDs were shallower by about 150 m than the predicted MLD (Figure 3e) but matched the depth of the deep thermocline. In addition, late winter deep mixed layers that reached 1700–1800 m in those boxes were colder than the water mass found at the same levels in August–September 2014 by about 0.15°C. The heat extracted from the ocean in those two boxes during the whole winter was used to deepen the mixed layers down to the top of the deep thermocline and to cool it.

A cooling of the upper part of the water column is observed between September 2014 and September 2015 in the three basins (Figure S2). It is consistent with the cold SST anomaly computed compared to the period 2000–2015 that was present in June 2015 over the whole subpolar gyre and that was attributed to the strong atmospheric forcing that prevailed during Winter15 [Duchez et al., 2016; *de Jong and de Steur*, 2016]. Interestingly, a cold SST anomaly of about 1–2°C was already present in the subpolar gyre in November 2014 [Duchez et al., 2016] and has likely favored the positive NAO phase observed in Winter15 as such SST anomaly was proven to influence the phase of the NAO [Hurrell and Deser, 2009; Scaife et al., 2014]. This cold anomaly was considered as a reemergence of subsurface anomaly from the preceding winter and was present down to 700 m (Figure S2; Duchez et al., 2016). Being not salinity compensated, it caused a density increase in the upper 700 m between September 2013 and September 2014 (not shown) and acted as a preconditioning of the water column for deep convection, especially in IRM. Indeed,  $HC_{ext}$  computed from 2013 summer conditions but with a heat loss of  $3 \times 10^9$  J as that observed in Winter15 suggests that MLDs would have only reached 800 m without the preconditioning by the cold anomaly (Figure 3e). The cold anomaly that developed recently in the subpolar gyre of the North Atlantic Ocean favored the intense Winter15 deep convection, which in turn enhanced this cold anomaly.

Despite the exceptional character of Winter15, which was similar in terms of atmospheric conditions to those of the early 1990s, deep convection in LAB was shallower during Winter15 than during the early 1990s winters when it reached 2400 m. To understand this difference, we computed  $HC_{ext}$  from summer profiles collected in 1993 and 1994 along the AR7W line in LAB [Yashayaev, 2007] (not shown). We found that, with similar air-sea heat loss, the vertical extent of the deep convection could be much larger in the early 1990s than in Winter15 because the deep thermocline lay at 2300–2400 m during this period. In addition, the heat loss required to deepen the mixed layers down to the deep thermocline depth in the early 1990s (about  $1 \times 10^9$  J) was much less than the observed heat loss (more than  $3 \times 10^9$  J) (Figure 4a). This would explain the LSW cooling trend observed in the early 1990s [Yashayaev, 2007].

## 5. Conclusions

During winter 2014–2015, a major deep convective activity forced by exceptional turbulent air-sea fluxes occurred over an area extending from the interior of the Labrador Sea to the Irminger Sea. It was favored by and enhanced the cold anomaly that developed recently in the subpolar gyre of the North Atlantic Ocean. The MLDs reached 1800 m in the Labrador Sea, which is similar to the deepest MLDs observed since the mid-1990s but shallower than those observed in the early 1990s. The MLDs reached 1700 m and 1400 m south of Cape Farewell and in the Irminger Sea, respectively, which are the deepest MLD directly observed in those two regions. The three basins formed LSW of same density but with different temperatures and salinities. In the Irminger Sea, the MLDs extended down to the base of the LSW pool (1400 m)

### Acknowledgments

We thank the reviewers for their constructive comments. Anne Piron and Virginie Thierry are funded by IFREMER (Institut Français de Recherche pour l'Exploitation de la Mer), Hélène Mercier is funded by CNRS (the French Centre National de la Recherche Scientifique), and Guy Caniaux is funded by Météo-France. This paper is a contribution to the EQUIPEX NAOS project funded by the French National Research Agency (ANR) under reference ANR-10-EQPX-40, to the AtlantOS project (H2020), to the OVIDE project supported by IFREMER, CNRS and INSU (Institut National des Sciences de l'Univers), and by French national programs (INSU/LFE). OVIDE is a contribution to CLIVAR. This study is also a contribution to the project BOCATS (CTM2013-41048-P) supported by the Spanish Ministry of Economy and Competitiveness (BES-2014-070449) and cofunded by the Fondo Europeo de Desarrollo Regional 2007–2012 (FEDER). This work benefitted from the French research infrastructures Euro-Argo and flotte (TGIR EuroArgo and TGIR flotte) and more specifically from the OVIDE cruises realized on board the French RV *Thalassa* and during which many Argo floats used in that study were deployed. Argo data were collected and made freely available by the International Argo Program and the national programs that contribute to it (<http://www.argo.ucsd.edu>, <http://argo.jcommops.org>). Argo data used in that study were downloaded from the Coriolis Data Center (<http://www.coriolis.eu.org>) and are listed in the references. Surface wind stress, air-sea heat flux, and SST were downloaded from the ERA-Interim website (<http://www.ecmwf.int/en/research/climate-reanalysis/era-interim>). Absolute Dynamic Topography data were downloaded from AVISO (Archiving, Validation, and Interpretation of Satellite Oceanographic data) web site (<http://www.aviso.oceanobs.com/duacs/>). Sea ice data were obtained from the Centre de Recherche et d'Exploitation Satellitaire (CERSAT), at IFREMER, Plouzané (France) (<http://cersat.ifremer.fr/data/products/catalogue>). ISAS maps [Gaillard et al., 2016] were downloaded from the ISAS viewer website (<http://www.umr-lops.fr/SO-Argo/Products/ISAS-T-S-fields/ISAS-viewer>).

[Daniault et al., 2016] so that the convective patches contributed to the renewal of the LSW over its full depth range. The mixed layer deepening in the Labrador Sea was limited by the deep thermocline density gradient, and a significant cooling of the LSW compared to previous year was observed. By contrast, the MLDs observed south of Cape Farewell and in the Irminger Sea nearly correspond to the MLDs predicted by applying surface fluxes to the end of summer heat content. We cannot exclude that such exceptional widespread deep convection occurred before, most likely in the early 1990s when winters were as exceptional as winter 2014–2015 and when convection intensity was at a maximum in the Labrador Sea [Yashayaev, 2007], but sparse observations prevent to confirm it. One may also wonder whether this enhanced LSW production was associated with an intensification of the MOC [Rahmstorf et al., 2015].

If harsh winters regularly occur in the future as observed since 2008, we can expect that the deep thermocline will continue to be eroded and cooled and that a new dense and cold LSW variety will be formed. Those changes in the strength of deep convection and on the properties of the LSW are not surprising in the subpolar gyre of the North Atlantic, which is known to have exhibited significant variability over the past five decades [Yashayaev, 2007]. However, we might also expect that reduced winter oceanic heat loss and increased inflow of freshwater from Greenland and the Nordic Seas in a warming world could modify the natural deep convection cycle [Yang et al., 2016; Brodeau and Koenigk, 2016] and impact the MOC [Rahmstorf et al., 2015]. Some climate model simulations even predicted the complete extinction of deep convection in the Labrador Seas after the 2020s [Brodeau and Koenigk, 2016]. In this context, using models with the Argo observations of deep convection as benchmarks could lead to better understanding of the role of the various parameters involved in deep convection, which is more than ever required to improve their representation in climate models.

### References

- Argo (2015), Argo float data and metadata from Global Data Assembly Centre (Argo GDAC)—Snapshot of Argo GDAC of May, 8th 2015. SEANOE, doi:10.17882/42182#42336.
- Bacon, S., W. J. Gould, and Y. Jia (2003), Open-ocean convection in the Irminger Sea, *Geophys. Res. Lett.*, 30(5), 1246, doi:10.1029/2002GL016271.
- Brodeau, L., and T. Koenigk (2016), Extinction of the northern oceanic deep convection in an ensemble of climate model simulations of the 20th and 21st centuries, *Clim. Dyn.*, 46, 2863–2882, doi:10.1007/s00382-015-2736-5.
- Cunningham, S. A., et al. (2007), Temporal variability of the Atlantic meridional overturning circulation at 26.5 N, *Science*, 317, 935–937.
- Daniault, N., et al. (2016), The northern North Atlantic Ocean mean circulation in the early 21st Century, *Prog. Oceanogr.*, 146, 142–158, doi:10.1016/j.pocean.2016.06.007.
- de Boisséson, E., V. Thierry, H. Mercier, and G. Caniaux (2010), Mixed layer heat budget in the Iceland Basin from Argo, *J. Geophys. Res.*, 115 C10055, doi:10.1029/2010JC006283.
- de Boyer Montégut, C., G. A. Madec, S. Fischer, A. Lazar, and D. Iudicone (2004), Mixed layer depth over the global ocean: An examination of profile data and a profile-based climatology, *J. Geophys. Res.*, 109, C12003, doi:10.1029/2004JC002378.
- de Jong, M. F., and L. de Steur (2016), Strong winter cooling of the Irminger Sea in winter 2014–15, exceptional deep convection, and the emergence of anomalously low SST, *Geophys. Res. Lett.*, 43, 1717–1734, doi:10.1002/2016GL069596.
- de Jong, M. F., H. M. van Aken, K. Våge, and R. S. Pickart (2012), Convective mixing in the central Irminger Sea: 2002–2010, *Deep Sea Res.*, I, 63(1), 36–51.
- Dee, D. P., et al. (2011), The ERA-Interim reanalysis: Configuration and performance of the data assimilation system, *Q. J. R. Meteorol. Soc.*, 137, 553–597, doi:10.1002/qj.828.
- Duchez, A., E. Frajka-Williams, S. A. Josey, D. G. Evans, J. P. Grist, R. Marsh, G. D. McCarthy, B. Sinha, D. I. Berry, and J. J.-M. Hirschi (2016), Drivers of exceptionally cold North Atlantic Ocean temperatures and their link to the 2015 European heat wave, *Environ. Res. Lett.*, 11, 7, doi:10.1088/1748-9326/11/7/074004.
- Fetterer, F., K. Knowles, W. Meier, and M. Savoie. 2016, updated daily. Sea Ice Index, Version 2, Natl. Snow and Ice Data Cent., Boulder, Colo., doi:10.7265/N5736NV7.
- Fröb, F., A. Olsen, K. Våge, G. Moore, I. Yashayaev, E. Jeansson, and B. Rajasakaran (2016), Irminger Sea deep convection injects oxygen and anthropogenic carbon to the ocean interior, *Nat. Commun.*, 7, 13,244, doi:10.1038/ncomms13244.
- Gaillard, F., T. Reynaud, V. Thierry, N. Kolodziejczyk, and K. von Schuckmann (2016), In-situ based reanalysis of the global ocean temperature and salinity with ISAS: Variability of the heat content and steric height, *J. Clim.*, 29, 1305–1323, doi:10.1175/JCLI-D-15-0028.1.
- Garcia, H. E., R. A. Locarnini, T. P. Boyer, J. I. Antonov, O. K. Baranova, M. M. Zweng, and D. R. Johnson (2010), in *World Ocean Atlas 2009, Volume 3: Dissolved Oxygen, Apparent Oxygen Utilization, and Oxygen Saturation*, NOAA Atlas NESDIS 70, edited by S. Levitus, U.S. Gov. Print. Off., Washington, D. C.
- Hurrell, J. W. (1995), Decadal trends in the North Atlantic Oscillation: Regional temperatures and precipitation, *Science*, 269, 676–679, doi:10.1126/science.269.5224.676.
- Hurrell, J. W., and C. Deser (2009), North Atlantic climate variability: The role of the North Atlantic Oscillation, *J. Mar. Syst.*, 78, 28–41, doi:10.1016/j.jmarsys.2008.11.026.//000268701200004.
- Kieke, D., and I. Yashayaev (2015), Studies of Labrador Sea Water formation and variability in the subpolar North Atlantic in the light of international partnership and collaboration, *Prog. Oceanogr.*, 132, 220–232, doi:10.1016/j.pocean.2014.12.010.
- Lazier, J., R. Hendry, A. Clarke, I. Yashayaev, and P. Rhines (2002), Convection and restratification in the Labrador Sea, 1990–2000, *Deep Sea Res.*, I, 49, 1819–1835.

- Lilly, J. M., P. B. Rhines, M. Visbeck, R. Davis, J. R. Lazier, F. Schott, and D. Farmer (1999), Observing deep convection in the Labrador Sea during winter 1994–1995, *J. Phys. Oceanogr.*, 29, 2065–2098.
- Mercier, H., P. Lherminier, A. Sarafanov, F. Gaillard, N. Daniault, D. Desbruyères, A. Falina, B. Ferron, T. Huck, and V. Thierry (2015), Variability of the meridional overturning circulation at the Greenland–Portugal OVIDE section from 1993 to 2010, *Prog. Oceanogr.*, 132, 250–261, doi:10.1016/j.pocean.2013.11.001.
- Pérez, F. F., H. Mercier, M. Vazquez-Rodríguez, P. Lherminier, A. Velo, P. Pardo, G. Roson, and A. Rios (2013), Reconciling air-sea CO<sub>2</sub> fluxes and anthropogenic CO<sub>2</sub> budgets in a changing North Atlantic, *Nat. Geosci.*, 6, 146–152, doi:10.1038/ngeo1680.
- Pickart, R. S., D. J. Torres, and R. A. Clarke (2002), Hydrography of the Labrador Sea during active convection, *J. Phys. Oceanogr.*, 32, 428–457.
- Pickart, R. S., F. Straneo, and G. W. K. Moore (2003a), Is Labrador Sea Water formed in the Irminger basin?, *Deep Sea Res., I*, 50, 23–52, doi:10.1016/S0967-0637(02)00134-6.
- Pickart, R. S., M. A. M. Spall, H. Ribergaard, G. W. K. Moore, and R. F. Milliff (2003b), Deep convection in the Irminger sea forced by the Greenland tip jet, *Nature*, 424, 152–156, doi:10.1038/nature01729.
- Piron, A., V. Thierry, H. Mercier, and G. Caniaux (2016), Argo float observations of basin-scale deep convection in the Irminger sea during winter 2011–2012, *Deep Sea Res., I*, 109, 76–90, doi:10.1016/j.dsr.2015.12.012.
- Rahmstorf, S., J. E. Box, G. Feulner, M. E. Mann, A. Robinson, S. Rutherford, and E. J. Schaffernicht (2015), Exceptional twentieth-century slowdown in Atlantic Ocean overturning circulation, *Nat. Clim. Change*, 5, 475–480, doi:10.1038/nclimate2554.
- Scaife, A. A., et al. (2014), Skillful long-range prediction of European and North American winters, *Geophys. Res. Lett.*, 41, 2514–2519, doi:10.1002/2014GL059637.
- Takeshita, Y., T. R. Martz, K. S. Johnson, J. N. Plant, D. Gilbert, S. C. Risner, C. Neill, and B. Tilbrook (2013), A climatology-based quality control procedure for profiling float oxygen data, *J. Geophys. Res. Oceans*, 118, 5640–5650, doi:10.1002/jgrc.20399.
- Thomson, R. E., and I. V. Fine (2003), Estimating mixed layer depth from oceanic profile data, *J. Atmos. Oceanic Tech.*, 20, 319–329, doi:10.1175/1520-0426(2003)020<0319:EMLDFO>2.0.CO;2.
- Våge, K., R. S. Pickart, G. W. K. Moore, and M. H. Ribergaard (2008), Winter mixed layer development in the central Irminger Sea: The effect of strong, intermittent wind events, *J. Phys. Oceanogr.*, 38, 541–565, doi:10.1175/2007JPO3678.1.
- Våge, K., R. S. Pickart, V. Thierry, G. Reverdin, C. M. Lee, B. Petrie, T. A. Agnew, A. Wong, and M. H. Ribergaard (2009), Surprising return of deep convection to the subpolar North Atlantic Ocean in winter 2007–2008, *Nat. Geosci.*, 2, 67–72, doi:10.1038/ngeo382.
- Våge, K., R. S. Pickart, A. Sarafanov, O. Knutsen, H. Mercier, P. Lherminier, H. M. van Aken, J. Meincke, D. Quadfasel, and S. Bacon (2011), The Irminger Gyre: Circulation, convection, and interannual variability, *Deep Sea Res., I*, 58(S), 590–614, doi:10.1016/j.dsr.2011.03.001.
- Yang, Q., T. H. Dixon, P. G. Myers, J. Bonin, D. Chambers, and M. R. van den Broeke (2016), Recent increases in Arctic freshwater flux affects Labrador Sea convection and Atlantic overturning circulation, *Nat. Commun.*, 7(10525), 2016, doi:10.1038/ncomms10525.
- Yashayaev, I. (2007), Hydrographic changes in the Labrador Sea, 1960–2005, *Prog. Oceanogr.*, 73, 242–276.
- Yashayaev, I., and J. W. Loder (2009), Enhanced production of Labrador Sea Water in 2008, *Geophys. Res. Lett.*, 36, L01606, doi:10.1029/2008GL036162.